#8 AU 6/26/01

IN THE UNITED STATES PATENT AND TRADEMARK OFFICE

In re Patent Application of:	)
	)
SKLAR *et al.*	)
	) **Art Unit: 1641**
Serial No.: 09/501,643	)
	) **Examiner: Gabel, G.**
Filed: February 10, 2000	)
	)
For: FLOW CYTOMETRY FOR HIGH THROUGHPUT SCREENING	)
	)**DOCKET NO: UNME-0070-1**

Director of the U.S. Patent and Trademark Office
Washington, D.C. 20231

REQUEST FOR PRIORITY
UNDER 35 U.S.C. § 120

Sir:

In the matter of the above-captioned application for a United States patent, notice is hereby given that the Applicant claims the priority date of November 9, 1999, the filing date of the Provisional Patent Application No. 60/156,946 under 35 U.S.C. § 120.

Respectfully submitted,

Ajay A. Jagtiani
Registration Number 35,205

JAGTIANI & ASSOCIATES
10379-B Democracy Lane
Fairfax, Virginia 22030
(703) 591-2664

June 21, 2001

A Flow Injection Flow Cytometry System for On-Line Monitoring of Bioreactors

Rui Zhao, Arvind Natarajan, Friedrich Srienc

Department of Chemical Engineering and Materials Science, Biological Process Technology Institute, University of Minnesota, 240 Gortner Lab, 1479 Gortner Avenue, St. Paul, MN 55108; telephone: (612)-624-9776; fax: 612-625-1700; e-mail: fried@cbs.umn.edu

Received 27 February 1998; accepted 9 September 1998

Abstract: For direct and on-line study of the physiological states of cell cultures, a robust flow injection system has been designed and interfaced with flow cytometry (FI-FCM). The core of the flow injection system includes a microchamber designed for sample processing. The design of this microchamber allows not only an accurate on-line dilution but also on-line cell fixation, staining, and washing. The flow injection part of the system was tested by monitoring the optical density of a growing *E.coli* culture on-line using a spectrophotometer. The entire growth curve, from lag phase to stationary phase, was obtained with frequent sampling. The performance of the entire FI-FCM system is demonstrated in three applications. The first is the monitoring of green fluorescent protein fluorophore formation kinetics in *E.coli* by visualizing the fluorescence evolution after protein synthesis is inhibited. The data revealed a subpopulation of cells that do not become fluorescent. In addition, the data show that single-cell fluorescence is distributed over a wid range and that the fluorescent population contains cells that are capable of reaching significantly higher expression levels than that indicated by the population average. The second application is the detailed flow cytometric evaluation of the batch growth dynamics of *E.coli* expressing Gfp. The collected single-cell data visualize the batch growth phases and it is shown that a state of balanced growth is never reached by the culture. The third application is the determination of distribution of DNA content of a *S. cerevisiae* population by automatically staining cells using a DNA-specific stain. Reproducibility of the on-line staining reaction shows that the system is not restricted to measuring the native properties of c lls; rather, a wider range of cellular components could be monitored after appropriate sample processing. The system is thus particularly useful because it operates automatically without direct operator supervision for extended time periods. © 1999 John Wiley & Sons, Inc. *Biotechnol Bioeng* **62**: 609–617, 1999.

Keywords: online flow cytometry; flow injection flow cytometry; automatic staining; bioreactor monitoring

INTRODUCTION

There is ample evidence that growing cells are heterogeneous entities that differ from one another in their physiological states. Microbial heterogeneity may arise due to phenotypic changes associated with the cell cycle (Dien and Srienc, 1991; Srienc and Dien, 1992), due to changes in the microenvironments of individual cells (Dunlop and Ye, 1990; Fowler and Dunlop, 1989), or due to mutations resulting in genotypic variations in the population (Hall, 1995). Thus, rates of growth-associated parameters, such as protein synthesis or substrate uptake, are distributed in the population. From a biochemical engineering perspective, these population dynamics have profound implications, because the overall productivity of the microbial process depends on the contribution of each individual cell. One method to estimate such dynamics is by the use of flow cytometry.

In a process environment, rapid, repeated, and long-term on-line manual analysis is usually impractical, if not impossible. Therefore, a certain degree of automation is desirable, particularly for more complex analysis procedures such as flow cytometry. To date, a number of flow injection systems have been designed and widely used in microbial process control and automatic analysis (Munch et al., 1992; Reed, 1990; Ruzicka and Hansen, 1975, 1988), but most of them monitor population-averaged properties. The concept of automatic flow cytometric analysis was introduced by Omann et al. (1985), who constructed a sample introduction device fitted to a Becton Dickinson FACS cytometer. Kelley (1989) also developed a similar device. Pennings et al. (1987) developed a system based on continuous pumping of cells and reagents with a peristaltic pump. Although the capabilities of these designs are rather limited, they are pioneering designs in automated flow cytometry. Successful on-line flow cytometry has been demonstrated using a flow injection technique (Ruzicka and Lindberg, 1992).

In this study, we present a flow injection system interfaced with a flow cytometer and a bioreactor to perform on-line assessment of single-cell property distributions. The versatility and performance of this system are demonstrated in several preliminary examples that show the utility of the system as it provides detailed quantitative information on growing cell populations that cannot be obtained with any other existing method.

Correspondence to: F. Srienc

CCC 0006-3592/99/060609-09

MATERIALS AND METHODS

Cell Strains, Growth Medium, Growth Conditions, and Staining Conditions

E. coli strain K12 was used in the growth experiment involving on-line monitoring of optical density. Cells were grown in 300 mL of 2XGYT complex medium (Sambrook et al., 1989) in a 1-L flask placed in a 30°C water bath and shaken at 225 rpm. The culture was aerated at 1 vvm by a peristaltic pump through an airstone (Cole-Parmer, Vernon Hills, IL) immersed in the medium. *E. coli* BL21 cells transformed with the plasmid pRSET/S65T (a kind gift from Dr. R. Y. Tsien, Howard Hughes Medical Center, San Diego) were used in the experiment to study the Gfp fluorophore formation kinetics and batch growth dynamics. The plasmid contains an ampicillin-resistance marker gene, and the Gfp gene under the control of a T7 RNA polymerase promoter. Cells were grown in LB complex medium containing ampicillin (100 μg/mL). Production of T7 RNA polymerase was regulated using an IPTG inducible *lacZ* promoter present in the host chromosome. IPTG (200 μg/mL) was used to induce Gfp expression, and chloramphenicol (30 μg/mL) was used to inhibit the protein synthesis when needed (Sambrook et al., 1989).

Saccharomyces cerevisiae strain YPH399a (*MATa, ade2-101, leu2Δ1, lys2-80, his3Δ200, trp1Δ63, ura3-52*) cells were grown overnight in 3 mL YPD medium (bacto-yeast extract 1% w/v, bacto-peptone 2% w/v, dextrose 2% w/v) at 30°C and 225 rpm in a 15-mL polystyrene test tube (Falcon). Cells were diluted to a concentration of ca. 1×10^6 cells in fresh medium, and the tube was placed on ice. Samples were automatically withdrawn into the microchamber of the flow injection system. Inside the microchamber, samples were washed with ice-cold PBS (0.15 *M*, pH 7.5), fixed in ice-cold 70% ethanol, washed with ice-cold PBS, treated with chromatin denaturation solution (0.1N HCl, 0.5% w/v Triton X-100, 1.75% w/v NaCl), washed with ice-cold PBS, and stained with mithramycin A (Sigma, 30 μg/mL in PBS, 2 m*M* $MgCl_2$). Fixation and denaturation steps were 2 min in length, washes were 1 min in length, and cells were stained with mithramycin for 10 min. Fixation, denaturation, and washing were performed by continuously pumping the appropriate reagent through the microchamber while mixing the suspended cells using a magnetic stir-bar.

FI-FCM System

The equipment used to construct the flow injection system is listed in Table I. The components were interfaced to a personal computer using DT2805 and DAS1601 data acquisition and system control boards through digital input/output (DI/O) and digital-to-analog (D/A) subsystems. Labtech NOTEBOOK software (Laboratories Technology Corp., Wilmington, MA) was used to control both boards. Figure 1 shows a schematic overview of this FI-FCM system, which consists of three subsystems: (i) sample delivery; (ii) sample handling; and (iii) sample injection and analysis.

Table I. List of equipment.

Equipment	Manufacturer	Control method
1. Ten-position switching valve, Model C25Z	Valco Instruments Co. Inc., Houston, TX	TTL output, DI/O port #1, DT2805
2. Two-way injection valve, Model C22Z	Valco	TTL output, DI/O port #1, DT2805
3. Three-way switching valve, Model 01367-72	Cole-Parmer, Vernon Hills, IL	Relay driven, DI/O port #0, DT2805
4. Peristaltic pump, 7520-50	Cole-Parmer	Current output, D/A port #1, DT2805 Board
5. Syringe pump, pump 22	Harvard Instrumentation, Harvard, MA	RS-232c
6. Peristaltic pump, 7520-20, 7520-30	Cole-Parmer, IL	Masterflex speed control unit
7. Magnetic Stir Plate, Model 120s	Fisher Scientific, Pittsburgh, PA	
8. LH fermentor, 2L	LH Fermentation, Hayward, CA	LH fermentor control unit
9. DT2805 data acquisition and system control board	Data Translation, Marlboro, MA	
10. DAS1601 data acquisition and system control board	Keithley Data Acquisition, Taunton, MA	
11. Computer, Vectra/66	Hewlett Packard	Interfaced with flow cytometer
12. Computer, 486/25c	Gateway 2000, N. Sioux City, SD	Interfaced with FI system

A sample delivery loop transferred the cell culture from a bioreactor to the flow injection system. A static degassing unit was designed to release air bubbles trapped in the sample (Fig. 2a), and sample was continuously recirculated in this loop. During sampling periods, the cell culture with air bubbles was allowed to accumulate in the glass tube, and a weak vacuum was applied using a peristaltic pump. Due to a combination of static hydraulic buoyancy force and the vacuum, air bubbles were rapidly eliminated from the medium through a 0.45-μm in-line filter. The degassed sample was then fed into the microchamber of the sample handling subsystem for further processing. The sample residence time in the delivery loop was minimized, because the environmental conditions (in particular, the aeration) in the tubing were not the same as those in the bioreactor. However, care was taken to avoid shear-induced damage of the sample that might result from the use of very high flow rates in the tubing. Hence, Cole-Parmer Masterflex silicon tubing (size #13, i.d. 0.75 mm) and a flow rate of 5 mL/min (0.19 m/s) were used, resulting in a residence time of 10.5 s.

The sample handling consists of a ten-position switching valve (#1, Table I) connected with a precise peristaltic pump

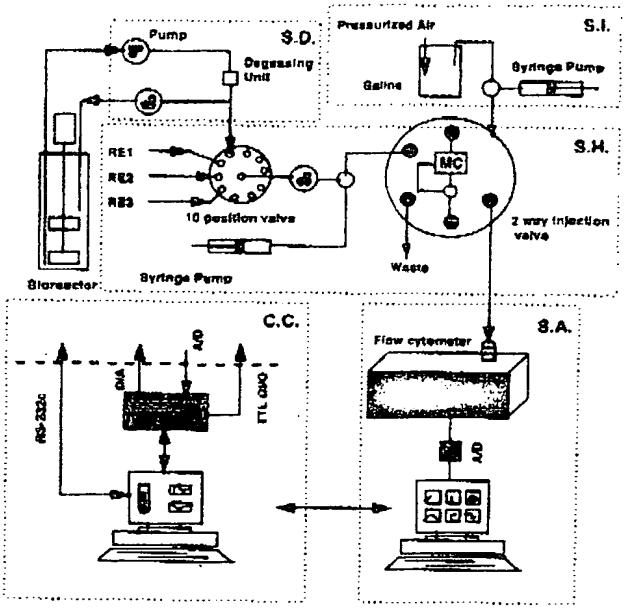

Figure 1. An overview of the FI-FCM system. The system consists of the following parts: sample delivery ("S.D."); sample handling ("S.H."); sample injection ("S.I."); sample analysis ("S.A."); and computer control ("C.C."). Sample from a bioreactor is first brought to a multiposition valve and degassing is performed. Up to 10 different samples or reagents ("RE1," etc.) can be selected and pumped into the system using the ten-position valve connected with a precise peristaltic pump. A microchamber ("MC") connected to a two-way injection valve is used to dilute samples or mix samples with different reagents. After treatment, samples are injected into the flow cytometer in a pulse-free manner by the mobile phase (saline), which is driven by pressurized air. The flow injection system is controlled by a PC through two data acquisition and system control boards. Flow cytometric data acquisition and analyses are performed by another PC.

(#4, Table I) to select up to ten different streams, and a two-way injection valve (#2, Table I) incorporated with a microchamber to load and inject samples (Fig. 2b,c). The key component in sample handling is the microchamber, which has been designed to allow on-line sample dilution and staining (Fig. 2d). The unit essentially represents a stirred-tank reactor with three ports that serve as inlets and outlets. Because dilution, staining processes, and other enzymatic reactions are basically mixing processes, they can be easily carried out in the microchamber in a predictable manner.

Ports A and B are directly connected to the microchamber, whereas port C is connected to the microchamber through an in-line filter. With this in-line filter, fluids can flow through the microchamber freely, but cells are retained inside. To load sample into the microchamber, outlet C is blocked (Fig. 2d), sample is pumped through microchamber from port A to port B. To perform on-line dilution of cell samples, water is pumped through the microchamber from port A to port B at a predetermined flow rate, F, for a certain time, t, such that the sample is diluted by a factor D given by:

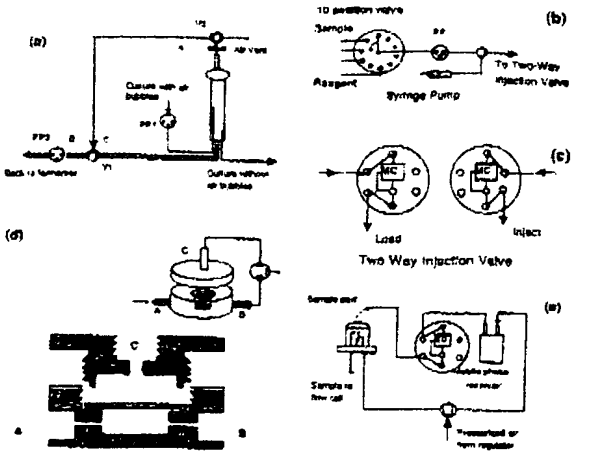

Figure 2. (a) The static degassing unit. Air bubbles trapped in the cell culture escape from the medium due to the buoyancy force enhanced by the weak vacuum provided by a peristaltic pump (PP2). (b, c) Schematic of sample handling subsystem. The center line of the ten-position switching valve is connected to a peristaltic pump (PP). Up to ten different streams can be fed into the system using this pump. The syringe pump (SP) is specifically assigned to perform on-line dilution, and to flush the system between samples. A microchamber (MC) is connected in the two-way injection valve. (d) Cross-sectional and three-dimensional views of the microchamber. Two side connections (A and B) allow fluids and cell particles to flow through, and the vertical connection (C) is separated from the microchamber through a membrane that allows only fluids to pass through. (e) Sample injection subsystem.

$$D(t) = \frac{C_0}{C(t)} = e^{(F/V)t} \qquad (1)$$

where V is the volume of the microchamber, and C_0 is the initial cell concentration. In practice, the volume term is modified to account for the dead volume of the connection tubing. To perform on-line staining, port C is opened, whereas port B is blocked. Solutions such as PBS or ethanol are pumped through the microchamber from port A to port C, so that cells inside the microchamber can be washed, fixed, and stained. After samples are processed, they are injected into the flow cytometer for analysis. The flow cytometer used was an Ortho Cytofluorograf IIs (Ortho Diagnostics Systems, Westwood, MA) equipped with an argon ion laser (Innova 90-5, Coherent Inc., Palo Alto, CA) and a Cicero data acquisition system (Cytomation, Fort Collins, CO). The laser was operated at 488 nm (Gfp) or 457 nm (mithramycin), and 100-mW beam power. A band-pass filter (525 ± 15 nm) and an OG530 long-pass filter were used to collect Gfp and mithramycin fluorescences, respectively. Data were acquired in listmode, pulse area, linear, and logarithmic configurations.

RESULTS

System Performance

To test the sample handling system, a growth study of *E.coli* cells was carried out using a spectrophotometer as the de-

tection device instead of a flow cytometer. The purpose of the experiment was to test the reliability of the sampling, degassing, and the dilution subsystems. A satisfactory performance of the system would yield the growth curve of a cell culture with frequent sampling points over the entire growth period by automatically carrying out dilutions to keep absorbance readings in the linear range when higher cell densities were reached.

The output transmittance signals of the spectrophotometer were acquired using the A/D subsystem of the DT2805 board. A typical output signal is shown in Figure 3a. The signal resembles a gamma distribution due to the dispersion of the sample in the carrier stream. The sample concentration was determined by integrating over the entire duration of the signal pulse. Because the dispersion of the cell culture within the carrier stream is not linearly related with the sample concentration, the recorded transmittance signals are not directly proportional to the sample concentration. This relationship can be described by the Taylor dispersion (Taylor, 1953) as follows:

$$C(t) = \frac{M/\pi R^2}{\sqrt{4\pi E\, t}}\, e^{-(Z-vt)^2/4Et} \tag{2}$$

where $C(t)$ is the concentration of the sample at the position of the detector at time t, M is the total amount of the sample injected into the carrier stream, E is the dispersion coefficient, R is the diameter of the tube, v is the velocity of the stream, and Z is the distance between the detector and the point of the injection. Transmittance $[V(t)]$ is related to cell concentration $[C(t)]$ according to Beer–Lambert's law (Zubay, 1993):

$$\log_{10}(V(t)) = -K\, d\, C(t) \tag{3}$$

where K is molar absorption coefficient, and d is the path length. Combining Eqs. (2) and (3), the following expression can be derived to relate the amount of sample to the measured transmittance signal:

$$\int_0^\infty (1 - \log V)\, dt \propto M \tag{4}$$

Eq. (4) is valid over the same linear range described by Beer–Lambert's law. This was determined to be the case for sample absorbances of <2.0 (Fig. 3b). Therefore, on-line dilutions were necessary for dense samples. A zero-order algorithm was used to calculate the dilution factor for the next sample ($D_i + 1$) based on the current concentration measurement (C_i) and the initial sample concentration (C_0). The algorithm:

$$D_{i+1} = C_i / C_0 \tag{5}$$

is valid when the frequency of sampling is greater than the frequency of cell division. The lag phase, exponential growth phase, and the stationary phase can be clearly recognized in the growth curve thus obtained (Figure 3c). On-line measurements showed very few variations associated with measurement errors, and measurements were thus stable and consistent. The on-line dilution started automatically 11 h after the start of the growth experiment, and dilution factors increased from 1 to 27 over the span of the experiment (Figure 3d). The degassing unit was able to efficiently remove air bubbles from the cell culture samples even during the late stages of the experiment when the cell culture was very dense (OD ~40). The two abnormal points shown in Figure 3a (at ca. 4 and 10 h) are probably due to air bubbles that likely originated from open ports on the ten-position switching valve. This potential problem can be avoided by sealing unused ports. One can note that the dilution factors calculated after the overshoots in the measurements did not diverge away, indicating that the zero-order algorithm is robust for this application.

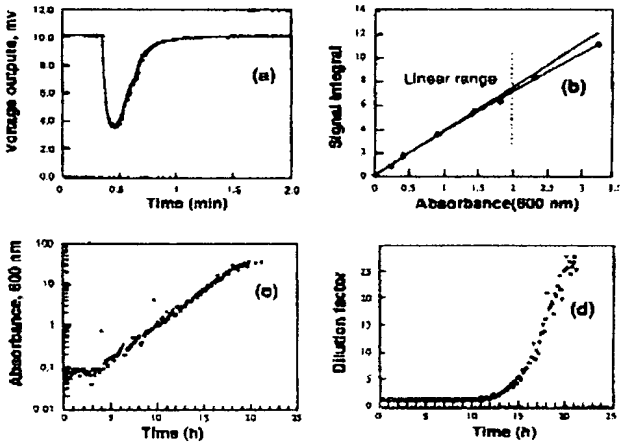

Figure 3. (a) Typical spectrophotometer output transmittance signal. The signal was acquired using the A/D subsystem of the DT2805 data acquisition board. (b) The range over which Beer–Lambert's law is valid was determined by diluting a dense culture, and measuring absorbance at 600 nm at each dilution. (c) *E. coli* growth curve. *E. coli* BL21 cells were grown in 2XGYT medium at 30°C, and the optical density of the cell culture was monitored on-line every 10 min for 22 h. The biomass doubling time was estimated as 1.77 h. (d) On-line dilution. On-line dilution started automatically 11 h after the start of the experiment, and the dilution factor increased to 27 over the course of the experiment.

Reproducibility of On-Line Flow Cytometry Measurements

A stable sample stream is very important to obtain accurate measurements on a flow cytometer. Hence, pressurized air was used to drive sample from the microchamber to the flow cytometer (Fig. 2e). Most FI systems, including some FI-FCM systems, use a mechanical syringe pump (Blankenstein et al., 1996; Lindberg et al., 1993). Using our syringe pump, it was found that the coefficient of variation of light-scatter distributions of calibration beads obtained was higher than 10% with strong concomitant background noise. In contrast, the use of pressurized air to drive samples gave reproducible, noise-free light-scatter distributions of calibration beads.

To test whether the on-line measurements indeed yield the correct distributions, replicates of light-scattering intensity distributions of *S. cerevisiae* cells measured on-line and off-line were compared (Figure 4a). It can be seen that the distributions obtained from on-line measurements can be superimposed over those from off-line measurements. The Kolmogorov–Smirnov (KS) statistical test (Neter et al., 1988) was performed to verify that the distributions can be considered statistically identical with a confidence level of >0.99. Thus, on-line measurements give the same information as off-line measurements.

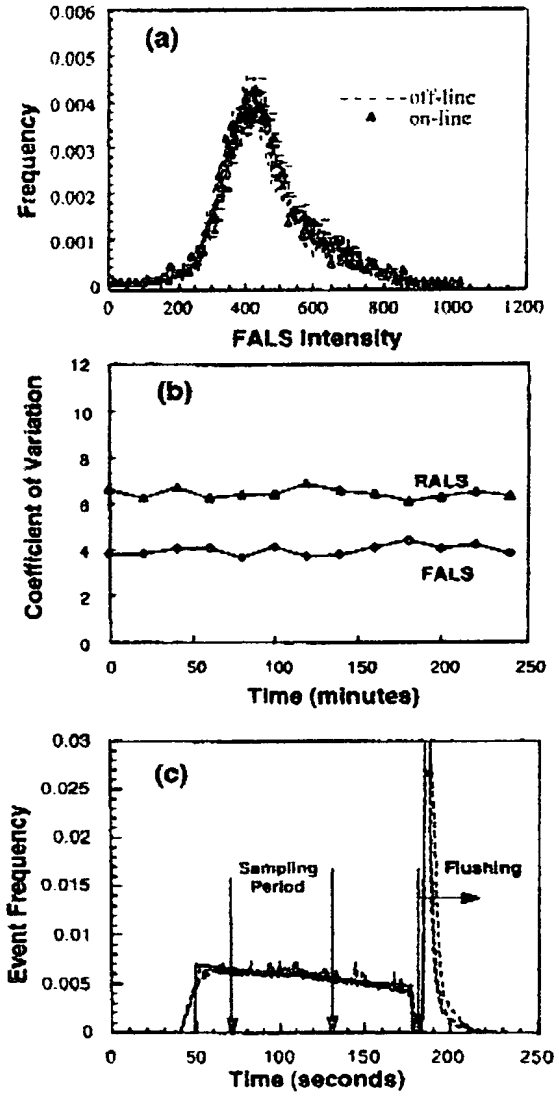

Figure 4. (a) Reliability. The light-scatter distributions of on-line and off-line measurements are compared to test the reliability of the on-line measurements. (b) Reproducibility. The coefficient of variation of forward- and right-angle light scatter (FALS and RALS) distributions of uniform calibration beads were measured over an extended time period to test the reproducibility of the on-line measurements. (c) Robustness. The time profiles of event frequencies of samples of various concentrations (400, 700, and 1700 events per second, dashed lines) were compared with an ideal profile that would be obtained in the absence of sample dispersion (solid lines). The "sampling period" (time window when samples are acquired) and "flushing period" of the sample analysis cycle are indicated.

Reproducibility of on-line measurements as a function of time was tested by comparing light-scattering intensity distributions of uniform calibration beads (2.013 ± 0.025 μm, Duke Scientific) measured every 10 min over a span of 4 h. Variance in light-scattering distributions of these beads is a useful indicator of the optical alignment of the flow cytometer. Hence, this measurement was used to estimate the stability of the on-line measurements. It was observed that the coefficient of variation (CV) of the distributions fluctuated very little over 4 h of periodic sampling (Figure 4b). A statistical analysis confirmed that the CVs were identical with 95% confidence (*t*-test; Neter et al., 1988), confirming that the measurements and the instrument settings were not subject to a drift over time.

The flow rate of samples that can be applied in a flow cytometer depends upon the sample concentration. The arrival of cells of a given concentration at the analysis point in the flow cytometer is governed by Poisson statistics. Hence, sample concentrations have to be adjusted to ensure that the probability of two or more cells being analyzed simultaneously is minimized. Here, a threshold of 1% was set for coincident events; that is, samples whose probability of coincidence of two or more cells exceeded 1% of the probability of single-event occurrence were diluted prior to analysis. The lower end of sample concentrations was determined by the minimum number of events desired for acquisition and the time available for sample collection. In our system, the working range of sample concentrations resulted in event flow rates between 100 and 1000 events per second. To examine whether samples whose concentrations varied in this working range were processed similarly, their time profiles (i.e., number of events as a function of time) were analyzed after sample injection for a range of concentrations. Under ideal circumstances with no sample dispersion, these profiles would be described by exponentially decaying functions with the specific rate of decrease equal to the dilution rate of samples out of the microchamber. The time profiles obtained experimentally were normalized to unit area to yield event-frequency profiles for ease of comparison, and they were found to be identical (Fig. 4c). This observation has several important implications. First, the window between the time of injection of sample and the time of analysis of sample was independent of the actual sample concentration. Second, the relative cell number density of the sample can be determined as the product of the number of events counted within a fixed time window (e.g., the "sampling period"; Fig. 4c) and the factor of dilution. Third, the actual profiles obtained were compared with the ideal profiles just described, and they were found to be very similar. After reaching a maximum less than 10 s after the sample front reaches the analysis point in the flow cytometer, event frequencies decreased, as de-

scribed by the ideal profile. This implies that the microchamber can indeed be approximated as an ideal stirred-tank reactor. Finally, any residual sample is completely flushed away during the flushing period, and hence there is no cross-contamination between successive samples. Thus, the system was robust in handling a range in cell concentrations, and yielded very reliable data.

Monitoring Cell Population Dynamics

To simplify the process, we initially measured native properties of cells. These are usually restricted to light-scatter intensity measurements. Whereas these parameters are very useful in discriminating cell populations and, in some cases, in estimating cell viability, they usually cannot be related directly to intrinsic quantitative biological properties of cells. Hence, we expressed the green fluorescent protein (Gfp) to obtain physiological data from which biological information can be directly inferred. Gfp is a naturally fluorescent protein that has been expressed in many heterologous hosts (Cubitt et al., 1995), and is a very useful reporter for quantitative, noninvasive detection of single-cell gene expression (Natarajan et al., 1998; Subramanian and Srienc, 1996). Gfp expression was induced by the addition of IPTG to exponentially growing *E. coli* cells. The objective of the experiment was to examine the heterogeneity in levels of protein expression in single cells in an exponentially growing population. Hence, protein synthesis was inhibited 5 min after induction by addition of chloramphenicol. Thus, expression of Gfp in all cells was restricted to a "pulse" of finite time. The time of induction is designated as time "0" in the graph shown in Figure 5. The culture was sampled and analyzed every 10 min using online flow cytometry after induction and inhibition of protein synthesis. On-line dilution was not performed because inhibition of protein synthesis resulted in growth arrest and the cell concentration remained constant. Figure 5a shows the time-evolution of the cellular fluorescence distribution. The population was initially nonfluorescent. After induction, the cells gradually increased in their fluorescence. The increase in the mean fluorescence value of the population (comparable to a population-averaged assay) is shown in Figure 5c ("100%"). The kinetics of increase in mean fluorescence are sigmoidal, possible because nascent Gfp molecules have to fold, cyclize, and oxidize the fluorophore sequentially prior to turning fluorescent. The increase in fluorescence saturates approximately 3 h postinduction. However, a significant fraction of the population remains nonfluorescent (20%, Fig. 5d). This subpopulation can be better visualized in the cytogram of FALS vs. fluorescence (Fig. 5b). In addition, there is significant heterogeneity in expression among fluorescent cells, indicating variability in the capacity to produce heterologous protein in the population. From a biotechnological process perspective, uniform maximal expression of protein is desirable among all cells in the population. One should note that this maximum expression level cannot be inferred from the mean of the entire heterogeneous population due to the presence of nonproducers and low-level producers. Rather, a single-cell assay of the kind described here is necessary. In the experiment just discussed, a choice of the top 10% or 5% of fluorescent cells indicates that this maximum capacity is three- or four-fold greater than the population average value (Fig. 5c).

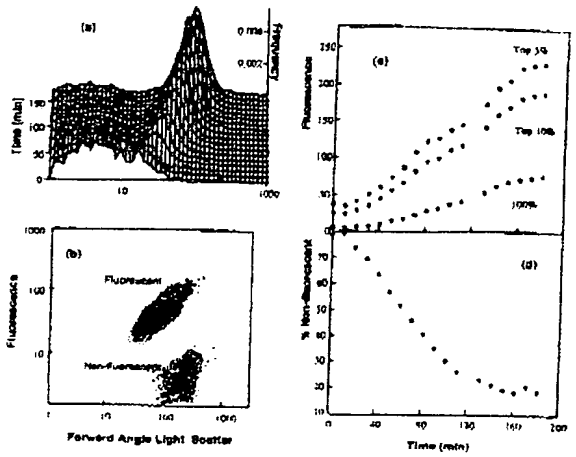

Figure 5. (a) The evolution of fluorescent populations. Green fluorescence intensity frequency distributions of the culture are plotted as a function of time. (b) The fluorescent population heterogeneity. A distinct population of nonfluorescent cells was observed. (c) The specific rate of increase of fluorescence of the top 5% and 10% fluorescent fractions is greater than the mean specific rate of the entire population. (d) The fraction of nonfluorescent cells was determined by comparing fluorescence intensity distributions of samples with those obtained from *E. coli* BL21 cells not expressing Gfp (negative control). The fraction decreased to a final value of ca. 20%. This population probably represents plasmid-free cells.

Monitoring Batch Growth Dynamics of *E. coli*

To test the system over longer time periods, the FI-FCM system was used to monitor the growth dynamics of *E. coli* cells from lag phase to stationary phase. On-line dilution up to 700-fold was performed over the course of growth. *E. coli* BL21 cells transformed with plasmid pRSET/S65T were grown at 37°C in complex medium containing ampicillin as a selection marker. Even though the culture was grown under noninducing conditions, uninduced "leaky" expression of Gfp was observed in the population. The cell culture was sampled and analyzed every 10 min, and forward-angle light scattering (FALS), right-angle light scattering (RALS), and fluorescence intensity signals were collected.

After a short lag phase of ca. 20 min, cells grew exponentially for 4 h, then entered stationary phase (Fig. 6a). The time evolution of the size (approximated by FALS intensity) distribution of growing *E. coli* culture from lag phase to stationary phase is shown (Fig. 6b). If the growth of cells was balanced, then frequency distributions of various properties such as cell size or protein content would be expected to be time-invariant. In the early exponential growth phase,

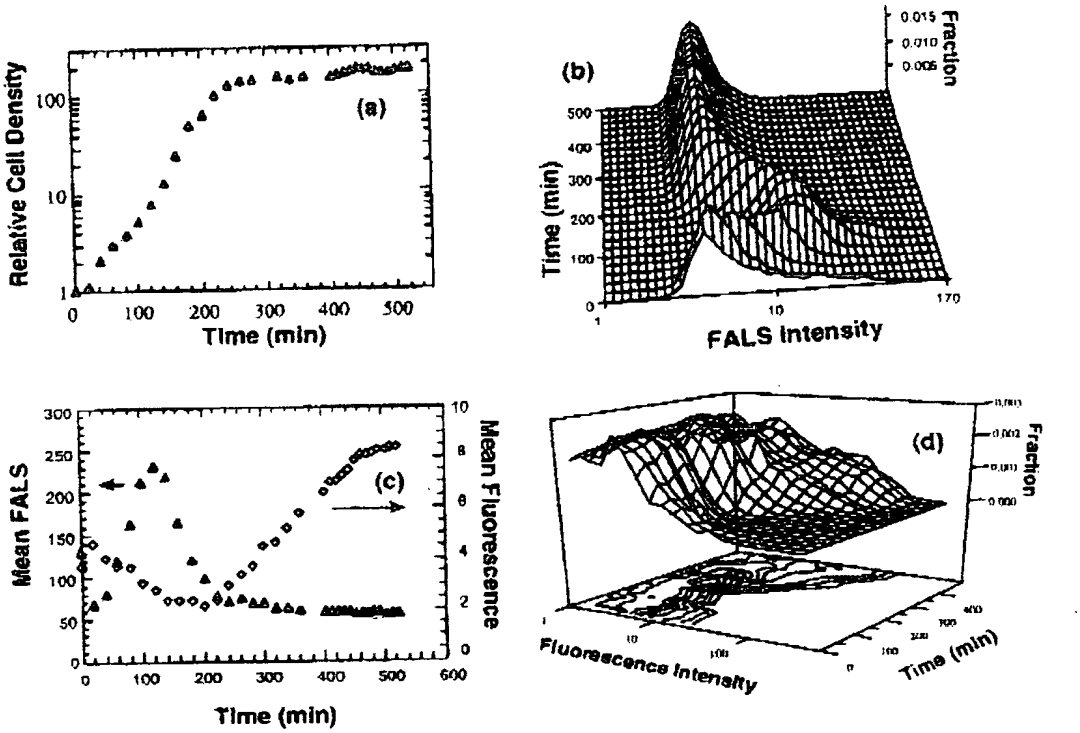

Figure 6. (a) The growth curve. The relative number density of the sample was measured by counting the number of cells analyzed during the sampling period and by setting the number density of the first sample to 1. (b) The size distribution of growing *E.coli* culture. The forward-angle light-scatter intensity was collected every 10 min to characterize the size distribution. (c) Mean intensities of light scatter (correlated with cell size: filled triangles) and fluorescence (open diamonds) of the population changed over the course of cell growth. During exponential growth, cell size increased while protein content decreased. The reverse trend was observed in the stationary phase. (d) The time evolution of the fluorescence intensity distributions is represented in isometric and contour plots. The majority of the cells were nonfluorescent during exponential growth. Cells became increasingly more fluorescent during late exponential/stationary phase, until, at the end of the experiment, two populations could be distinguished.

the peak of the FALS distribution shifted to right (indicating an increase in mean cell size), reached a maximum value, shifted back to lower mean intensity during late exponential growth. A similar trend is observed in the mean FALS signal intensity (Fig. 6c). Thus, growth was exponential, but not balanced. FALS intensity distributions were unchanged during the stationary phase. The fluorescence intensity distribution of the growing culture was also monitored. Although Gfp synthesis was not induced, there was sufficient "leaky" expression of the protein for the fluorescence to be detectable. Interestingly, heterogeneity of expression was observed even among uninduced cells (Fig. 6d). Levels of "leaky" uninduced expression were seen to be inversely correlated to the growth phase, as lag- and stationary-phase cells were more fluorescent than exponentially growing cells (Fig. 6c). Additionally, protein content distributions in the population also changed with time during the exponential growth period, further indicating that growth was unbalanced, as a time-invariant physiological state is never reached.

Monitoring Cell Cycle Distribution of *S. cerevisiae*

To demonstrate the staining capability of the FI-FCM system, DNA contents of *S. cerevisiae* cells were measured on-line as described earlier. Even the application of a simple, single stain requires multiple preparatory steps during which cell samples might potentially be lost. To eliminate this possibility, a 0.2-μm in-line filter was used to retain cells while they were treated with various chemicals. The flow through port C was analyzed for presence of cells after each step to ensure the integrity of the membrane. Membrane clogging, frequently a problem in many membrane systems, was virtually eliminated in our design because of coexisting tangential flow between ports A and B, continuous vigorous stirring in the microchamber, and dilution of cells to a concentration of ca. 10^5/mL prior to initiation of staining. Vigorous stirring also ensured that cells did not clump together during the fixation step.

To demonstrate staining capability, replicates of a sample of *S. cerevisiae* cells in late exponential phase were washed, fixed, treated with chromatin denaturation solution, stained with mithramycin (MI), and analyzed on the FCM. An asynchronous population would be expected to have a bimodal DNA distribution, where the two modes correspond to cells in G1 and G2 cell cycle phases, and this was observed (Fig. 7b). Because the culture was in late exponential/early stationary phase, a majority of the cells were observed in the

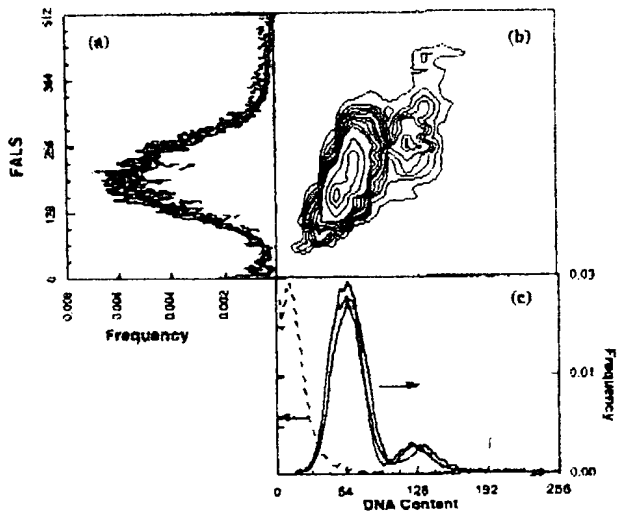

Figure 7. (b) A bivariate histogram of DNA content and forward-angle light-scatter intensity (FALS) of a late exponential *S. cerevisiae* culture. The two subpopulations observed correspond to cells in the G1 and G2 cell cycle phases. (c) DNA content distribution of three replicate samples of *S. cerevisiae* cells (solid line, Y2 axis) are compared with autofluorescence measurements of a fixed but unstained population (dashed line, Y1 axis). DNA distributions were obtained by staining with MI (see text). All distributions are normalized to unit area for ease of comparison. Autofluorescence distribution (shown on a slightly different scale) is clearly unimodal, and well separated from DNA distributions. (a) However, staining does not affect light-scatter intensity measurements, and FALS distributions of stained and unstained *S.cerevisiae* cells are identical.

G1 phase (Fig. 7c). DNA distributions obtained were compared with autofluorescence measurements on fixed and denatured cells that had not been stained. Autofluorescence distribution is clearly unimodal, and well separated from the stained distributions (Fig. 7c). In comparison, staining did not affect light-scatter intensity measurements, hence FALS distributions of unstained and stained cells were identical (Fig. 7a). DNA distributions for three replicate samples were also found to be statistically identical, ensuring reproducibility of the staining process (KS test; Neter, 1988). Because the entire process is automated, it is easy to envision the use of more complicated staining protocols to tag and quantitate other cellular components also.

DISCUSSION

To determine the state of a growing cell culture, conventional monitoring systems typically evaluate measurable quantities of the abiotic phase from which the state of the culture is inferred. Direct measurement of the physiological state is usually not possible because quantitative methods to rapidly assay the composition of the biomass are limited. Furthermore, the properties of individual cells are different and distributed over a range of physiological states. Therefore, population average data provide only limited information, and accurate information must be sought at the single-cell level.

Fredrickson et al. (1967) and Ramkrishna et al. (1968) proposed a general mathematical framework, known as population balance theory, to describe cell growth and its interaction with the environment (see also Ramkrishna, 1979, 1985). In this theory, the state of individual cells is specified by the physiological state vector—a collection of state properties such as cell size, protein content, or DNA content. The resulting population balance equations are essentially number balances on individual cells of a population, which keep track of, not only the generation and disappearance of cells, but also of the continuous change in the identity of cells due to physiological growth processes. This modeling framework (known as corpuscular and structured) most realistically represents the evolution of a heterogeneous microbial population. Versions of this model have been used to extract growth parameters from single-cell property distributions obtained using flow cytometry (Dien and Srienc, 1991; Kromenaker and Srienc, 1991, 1994a–c). However, these analyses were performed off-line for special cases. In general, it has been difficult to apply the population balance model to real microbial processes due to lack of experimental data that would permit identification of model parameters. Such data could possibly be generated by flow cytometry interfaced with appropriate instrumentation for on-line sample processing and analysis.

Hence, we designed and constructed a versatile and modular flow injection–flow cytometry (FI-FCM) system. To display the details of information that can be obtained, the system was used to monitor the heterogeneity of protein expression in an *E.coli* cell population. The results clearly reveal the need for single-cell analysis, because cellular content of even a single component such as Gfp content was distributed in the population. Frequent, automated sampling permitted observation of smooth trends of cellular phenomena. These data could be used to generate accurate estimates of the kinetics of transient events. Furthermore, it has been shown that the system can be used to monitor long-term fermentation processes, during the course of which cell concentrations would change significantly. Because the system does not require any operator intervention, it is particularly suitable for process monitoring and control applications. The data obtained can be used to determine not only specific rates of exponential growth, but also to determine the detailed physiological state distribution of the cell population. Additionally, single-cell growth parameters can be evaluated. To better define the composition of single cells, the range of cellular components that can be monitored can be expanded by taking advantage of the design of our microchamber, which permits on-line cell fixation, and staining, as we have demonstrated.

The examples presented demonstrate that the developed system represents a powerful tool for studying cell physiology at a level of detail that was not previously possible. Moreover, the FI-FCM system will be advantageous for monitoring bioreactors in studies involving transient growth phenomena, estimation of cellular kinetics, or study of synchronous or cyclic trends that might not be observed with

infrequent sampling. The system thus has significant potential in biotechnology for the monitoring of microbial populations, without the need for excessive manual intervention.

This work was supported partially by the National Science Foundation (BES-9708146) and by a seed grant from the Biological Process Technology Institute, University of Minnesota.

References

Blankenstein G, Scampavia LD, Ruzicka J, Christian GD. 1996. Coaxial flow mixer for real-time monitoring of cellular responses in flow injection cytometry. Cytometry 25:200–204.

Cubitt AB, Heim R, Adams SR, Boyd AE, Gross LA, Tsien RY. 1995. Understanding, improving and using green fluorescent proteins. Trends Biochem Sci 20:448–455.

Dien BS, Srienc F. 1991. Bromodeoxyuridine labeling and flow cytometric identification of replicating Saccharomyces cerevisiae cells: Lengths of cell cycle phases and population variability at specific cell cycle positions. Biotechnol Prog 7:291–298.

Dunlop EH, Ye SJ. 1990. Micromixing in fermentors: Metabolic changes in Saccharomyces cerevisiae and their relationship to fluid turbulence. Biotechnol Bioeng 36:854–864.

Fowler G, Dunlop EH. 1989. Effects of reactant heterogeneity and mixing on catabolite repression in cultures of Saccharomyces cerevisiae. Biotechnol Bioeng 33:1039–1046.

Fredrickson AG, Ramkrishna D, Tsuchiya HM. 1967. Statistics and dynamics of procaryotic cell populations. Math Biosci 1:327–374.

Hall BG. 1995. Adaptive mutations in Escherichia coli as a model for the multiple mutational origins of tumors. Proc Natl Acad Sci USA 92: 5669–5673.

Kelley KA. 1989. Sample station modification providing on-line reagent addition and reduced sample transit time for flow cytometers. Cytometry 10:796–800.

Kromenaker SJ, Srienc F. 1991. Cell-cycle-dependent protein accumulation by producer and nonproducer murine hybridoma cell lines. A population analysis. Biotechnol Bioeng 38:665–677.

Kromenaker SJ, Srienc F. 1994a. Cell cycle kinetics of the accumulation of heavy and light chain immunoglobulin proteins in a mouse hybridoma cell line. Cytotechnology 14:205–218.

Kromenaker SJ, Srienc F. 1994b. Effect of lactic acid on the kinetics of growth and antibody production in a murine hybridoma: Secretion patterns during the cell cycle. J Biotechnol 34:13–34.

Kromenaker SJ, Srienc F. 1994c. Stability of producer hybridoma cell lines after cell sorting: A case study. Biotechnol Prog 10:299–307.

Lindberg W, Ruzicka J, Christian GD. 1993. Flow injection cytometry: A new approach for sample and solution handling in flow cytometry. Cytometry 14:230–236.

Munch T, Sonnleitner B, Fiechter A. 1992. The decisive role of the Saccharomyces cerevisiae cell cycle behaviour for dynamic growth characterization. J Biotechnol 22:329–351.

Natarajan A, Subramanian S, Srienc F. 1998. Comparison of mutant forms of the green fluorescent protein as expression markers in Chinese hamster ovary (CHO) and Saccharomyces cerevisiae cells. J Biotechnol 62:29–45.

Neter J, Wasserman W, Whitmore GA. 1988. Applied statistics. 3rd edition. Boston: Allyn and Bacon.

Omann GM, Coppersmith W, Finney DA, Sklar LA. 1985. A convenient on-line device for reagent addition, sample mixing, and temperature control of cell suspensions in flow cytometry. Cytometry 6:69–73.

Pennings A, Speth P, Wessels H, Haanen C. 1987. Improved flow cytometry of cellular DNA and RNA by on-line reagent addition. Cytometry 8:335–338.

Ramkrishna D. 1979. Statistical models of cell population. In: Ghose TK, Fiechter A, Blakerbrough N, editors. Advances in biochemical engineering. New York: Springer. p 47.

Ramkrishna D. 1985. The status of population balances. Rev Chem Eng 3:49–95.

Ramkrishna D, Fredrickson AG, Tsuchiya HM. 1968. On relationships between various distributions functions in balanced unicellular growth. Bull Math Biophys 30:319–323.

Reed AL. 1990. Flow injection analysis in bioprocess control. Bioprocess Technol 6:221–241.

Ruzicka J, Hansen EH. 1975. Flow injection analysis. Anal Chim Acta 78:145–163.

Ruzicka J, Hansen EH. 1988. Flow injection analysis. 2nd edition. New York: Wiley.

Ruzicka J, Lindberg W. 1992. Flow injection cytoanalysis. Anal Chem 64:537–544.

Sambrook J, Maniatis T, Fritsch EF. 1989. Molecular cloning: A laboratory manual. 2nd edition. Cold Spring Harbor, NY: Cold Spring Harbor Laboratory Press.

Srienc F, Dien BS. 1992. Kinetics of the cell cycle of Saccharomyces cerevisiae. Ann NY Acad Sci 665:59–71.

Subramanian S, Srienc F. 1996. Quantitative analysis of transient gene expression in mammalian using the green fluorescent protein. J Biotechnol 49:137–151.

Taylor G. 1953. Dispersion of soluble matter in solvent flowing slowly through a tube. Proc R Soc Lond (Ser A) 219:186.

Zubay G. 1993. Biochemistry. Melbourne, Australia: William Brown.